

# Non-destructive detection of chicken freshness based on multiple features image fusion and support vector machine

Xiuguo Zou<sup>1\*</sup>, Chengrui Xin<sup>2</sup>, Chenyang Wang<sup>1</sup>, Yuhua Li<sup>1</sup>, Shuchen Wang<sup>3</sup>,  
Wentian Zhang<sup>4</sup>, Jiaojiao Li<sup>4</sup>, Steven Su<sup>4</sup>, Maohua Xiao<sup>2</sup>

(1. College of Artificial Intelligence, Nanjing Agricultural University, Nanjing 210031, China;

2. College of Engineering, Nanjing Agricultural University, Nanjing 210095, China;

3. School of Electrical and Control Engineering, Xuzhou University of Technology, Xuzhou 221018, China;

4. Faculty of Engineering and Information Technology, University of Technology Sydney, NSW 2007, Australia)

**Abstract:** With the rise in global meat consumption and chicken becoming a principal source of white meat, methods for efficiently and accurately determining the freshness of chicken are of increasing importance, since traditional detection methods fail to satisfy modern production needs. A non-destructive method based on machine vision and machine learning technology was proposed for detecting chicken breast freshness. A self-designed machine vision system was first used to collect images of chicken breast samples stored at 4°C for 1-7 d. The Region of Interest (ROI) for each image was then extracted and a total of 700 ROI images were obtained. Six color features were extracted from two different color spaces RGB (red, green, blue) and HSI (hue, saturation, intensity). Six main Gray Level Co-occurrence Matrix (GLCM) texture feature parameters were also calculated from four directions. Principal Component Analysis (PCA) was used to reduce the dimension of these 30 extracted feature parameters for multiple features image fusion. Four principal components were taken as input and chicken breast freshness level as output. A 10-fold cross-validation was used to partition the dataset. Four machine learning methods, Particle Swarm Optimization–Support Vector Machine (PSO-SVM), Random Forest (RF), Gradient Boosting Decision Tree (GBDT), and Naive Bayes Classifier (NBC), were used to establish a chicken breast freshness level prediction model. Among these, SVM had the best prediction effect with prediction accuracy reaching 0.9867. The results proved the feasibility of using a detection method based on multiple features image fusion and machine learning, providing a theoretical reference for the non-destructive detection of chicken breast freshness.

**Keywords:** chicken freshness, color space, gray level co-occurrence matrix, multiple features image fusion, machine learning

**DOI:** [10.25165/ij.ijabe.20241706.8783](https://doi.org/10.25165/ij.ijabe.20241706.8783)

**Citation:** Zou X G, Xin C R, Wang C Y, Li Y H, Wang S C, Zhang W T, et al. Non-destructive detection of chicken freshness based on multiple features image fusion and support vector machine. *Int J Agric & Biol Eng*, 2024; 17(6): 264–272.

## 1 Introduction

Compared with other common meat sources such as pork, beef, and lamb, chicken has the advantages of providing high protein and low fat, as well as high unsaturated fatty acids, minerals, and vitamins<sup>[1]</sup>. Chicken also provides a critical alternative meat source for individuals who are allergic or intolerant to red meat. Chicken is, therefore, a staple part of meat consumption globally, with a growth rate of more than 4% per annum in the past years<sup>[1]</sup>.

Currently, three types of raw chicken products are available on the market: fresh chicken, chilled chicken, and frozen chicken. Chilled chicken refers to chicken meat that passes quarantine inspection and is then slaughtered, whose central temperature is reduced to 8°C within 1 h after cooling but without quick freezing treatment, and reduced to 4°C within 12 h. Chilled chicken is required to be packed, stored, transported, and sold at 0°C–4°C<sup>[2]</sup>. Compared with fresh chicken and frozen chicken, chilled chicken provides better taste, flavor, freshness, and nutrition, and is also more convenient to manage in terms of hygiene and safety<sup>[3]</sup>. However, chilled chicken is highly perishable. The actions of enzymes and bacteria during meat storage processes will cause proteins, fat, and sugars in chicken meat to decompose and deteriorate, resulting in declining meat quality.

Consumers usually derive their first impression of food quality from its appearance. For meat products, color and texture are the most important appearance features. These two indicators are most likely to be used by consumers to make judgments on the quality, freshness, and nutritional value of meat. It has been shown that the color and texture of meat products could affect or even determine the consumers' purchase desire<sup>[4]</sup>. Methods to efficiently and accurately assess meat surface conditions are therefore essential for maintaining a stable meat supply and consumption chain. However, traditional evaluation methods require professional operators to perform destructive testing on chicken meat, which is time-

**Received date:** 2024-01-07 **Accepted date:** 2024-10-21

**Biographies:** Chengrui Xin, M.E., research interest: poultry phenotype, Email: [2021112042@stu.njau.edu.cn](mailto:2021112042@stu.njau.edu.cn); Chenyang Wang, M.E., research interest: poultry phenotype Email: [2020812083@stu.njau.edu.cn](mailto:2020812083@stu.njau.edu.cn); Yuhua Li, PhD, Lecturer, research interest: poultry phenotype and plant phenotype, Email: [lyhresearch@njau.edu.cn](mailto:lyhresearch@njau.edu.cn); Shuchen Wang, Professor, research interest: mechatronics and automation, Email: [wsc1967@xzit.edu.cn](mailto:wsc1967@xzit.edu.cn); Wentian Zhang, PhD, Research Associate, research interest: machine learning, deep learning, and signal processing, Email: [wentian.zhang@alumni.uts.edu.au](mailto:wentian.zhang@alumni.uts.edu.au); Jiaojiao Li, Senior Lecturer, research interest: biomedical engineering, Email: [Jiaojiao.Li@uts.edu.au](mailto:Jiaojiao.Li@uts.edu.au); Steven Su, PhD, Professor, research interest: biomedical instrumentation, physiological system modeling, Email: [Steven.Su@uts.edu.au](mailto:Steven.Su@uts.edu.au); Maohua Xiao, PhD, Professor, research interest: intelligent agricultural machinery, Email: [xiaomaohua@njau.edu.cn](mailto:xiaomaohua@njau.edu.cn).

\*Corresponding author: Xiuguo Zou, PhD, Associate Professor, research interest: poultry phenotype and inspection robot, College of Artificial Intelligence, Nanjing Agricultural University, No.1 Weigang, Nanjing 210095, China. Tel: +86-25-58606585, Email: [zouxiguoguo@njau.edu.cn](mailto:zouxiguoguo@njau.edu.cn).

consuming, susceptible to individual variation, and a waste of chicken meat. Such methods can no longer meet modern needs for rapid and accurate detection of meat freshness<sup>[5]</sup>. In the current environment that mandates strict food quality and safety regulations, there is an urgent need for an efficient, non-destructive, and accurate detection method for the freshness of meat products. Much research has been conducted in recent years to solve this problem, among which one of the most effective approaches is to introduce visual technology into the quality inspection of meat products.

Using machine vision can achieve non-destructive testing. Machine vision is a non-destructive detection technology that acquires information related to the quality of the objects being measured and then achieves rapid and accurate intelligent detection using the input information. Compared with traditional detection methods, machine vision technology provides many advantages, including rapid response, reduced susceptibility to interference from external factors, simple operation, and low cost<sup>[6]</sup>. In recent years, machine vision technology has been widely applied in the agricultural and food industries for various processes such as quality inspection, species identification, and online grading of agricultural and livestock products such as fruits<sup>[7,8]</sup>, vegetables<sup>[9,10]</sup>, meat<sup>[11,12]</sup>, and dairy products<sup>[13,14]</sup>. In the meat industry, visual technology is emerging as a new and potentially more effective method for detecting meat freshness<sup>[15,16]</sup>, tenderness<sup>[17,18]</sup>, pH<sup>[19]</sup>, and other features. For instance, Sun et al. predicted the color attributes of pork by extracting 18 color features from sample images using three-color space, RGB, HSI, and Lab, and establishing a linear regression model and stepwise regression model<sup>[20]</sup>. Barbin et al. developed a rapid evaluation method for chicken quality using a computer vision system by establishing a set of image color recognition frameworks based on the RGB model and quantitatively associating digital image information with color features measured by a colorimeter<sup>[21]</sup>. In recent years, hyperspectral imaging (HSI) has been increasingly used in the non-destructive detection of meat product nutritional value<sup>[22]</sup>, freshness, and other qualities<sup>[23]</sup>. In these studies, HSI was used to analyze the differences in chemical composition and physical features of food, as well as detect and compare the differences in spectral signals such as absorption, dispersion, reflectivity, and electromagnetic energy of specific wavelengths. However, because of the large amount of information contained in hyperspectral images, data processing steps are complex and time-consuming, so HSI struggles to meet the practical needs of industrial production lines.

Recently, convolutional neural network (CNN) technology has been applied in research on non-destructive testing of food. However, deep learning has higher requirements for the number of training sets and the computing power of the equipment. For practical applications, using image processing combined with machine learning provides better operability than CNN technology. A number of research studies have used this approach, but they mostly focus on the color information of meat<sup>[20,21]</sup>. However, the extraction of color information is easily affected by changes in external and environmental factors such as light intensity and camera shooting angle. Moreover, uncontrollable variations in slaughtering processes, such as bloodletting operations, will also affect the color of meat and reduce the accuracy of results. To increase accuracy, supplementing the color feature with texture features can allow a more comprehensive evaluation of the image features of the food.

Up to now, there is limited research on the rapid non-destructive detection of chicken freshness by fusing color

information with texture information. Using chicken breast samples, our study contributes to this research area by 1) building a machine vision system for collecting sample image information; 2) extracting the color features of samples from two different color spaces (RGB and HSI), and extracting Gray Level Co-occurrence Matrix (GLCM) texture features; and 3) establishing four different machine learning models for predicting chicken breast freshness levels, based on the correlation between color and texture features, and comparing the prediction effects provided by each model<sup>[24]</sup>.

## 2 Materials and methods

### 2.1 Data acquisition

Chicken breast fillets were acquired from a local market in Jiangbei New Area, Nanjing, China. The test samples were taken from the same breed of white-feathered broilers slaughtered within the same day and period in the standard slaughter line to avoid the influence of various objective conditions on meat quality during the slaughter process. The samples were placed in a constant temperature chamber after slaughter and brought back to the laboratory within 2 hours. The nodular tissue of chicken breast meat was removed on a sterile laboratory platform. A total of 35 sample blocks with approximate sizes of 3 cm×3 cm×1 cm were cut with a sterile knife<sup>[25]</sup> within one hour. Cut samples were placed in different sample boxes, labeled, and stored in a 4°C thermostat-regulated refrigerator for 7 d. Previous research using physical and chemical testing methods has developed classifications for the freshness levels of chicken stored for different periods under constant temperature and humidity conditions. Chicken freshness level is usually determined by the content of TVB-N and other ingredients, which change with storage time in a 4°C environment<sup>[24]</sup>. In this study, the freshness level of chicken breast samples stored at a constant temperature of 4°C was classified as Level 1 for 1-3 d, Level 2 for 4-5 d, and Level 3 for 6-7 d.

A self-designed machine vision system was used to collect images of chicken samples, as shown in Figure 1. The system consists of a wooden box, a light source, an industrial camera, and a computer. The box was made from wooden boards and an aluminum frame with a size of 40 cm×40 cm×60 cm. The internal walls of the box were covered with a black opaque photographic cloth to reduce interference from the background. The light source was a 12 W LED ring (outer diameter 26 cm, inner diameter 20 cm), and a 600 W pixel color camera (MV-CA060-10GC, Hikvision) was used for image acquisition. A 16 mm Factory Automation (FA) lens (MVL-HF1628M-6MP, 1/1.8, Hikvision) was used for the camera lens, and a CPL polarizing lens was added to this lens to reduce reflection. The camera properties were set to International Standards Organization (ISO) 640, exposure time 1/25 s, focal length 16 mm, and aperture 1.6.

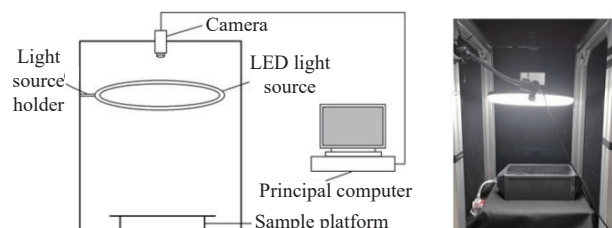


Figure 1 Schematic and photograph of machine device set-up

During the image acquisition process, the chicken breast sample was first placed in the sample chamber, the lens was focused to obtain a clear image, and the focusing knob was fixed using the

fixing bolt on the lens. The distance between the lens and sample was kept unchanged during image acquisition. Then, the image acquisition of each sample began, and images were collected and saved<sup>[25]</sup>. The image acquisition lasted for 7 d, and one image acquisition of all samples was completed in a fixed period each day. A total of 245 data were obtained.

**2.2 Dataset production**

**2.2.1 Image processing**

When using a camera for image acquisition, the brightness of the image generated by the cathode ray tube is affected by the input voltage. The signal in the dark area is lower than the actual intensity, while the signal in the bright area is higher than the actual darkened signal. Therefore, to reconstruct the real picture captured by the camera, it is necessary to use gamma correction for compensation processing in the later stage. Gamma correction involves editing the gamma curve of an image, using non-linear tone editing to identify dark and light areas in the image signal, and increasing their ratio to improve image contrast and restore the true information of the image. In this study, the MVS software from Hikvision Corporation was used to perform online gamma correction on images.

Image preprocessing is an important part of visual technology applications, aimed at removing interference information from the device itself and other external factors on the image, so as to obtain more accurate image information for subsequent feature extraction steps. This study mainly includes gamma correction of images, and the extraction of regions of interest (ROI). After the 3072×2048 pixels original images were collected, these images were imported into MATLAB (MATLAB R2017A, The MathWorks, Natick, MA, USA) for image processing. Before extracting image data, several ROIs with a size of 150×150 pixels were first defined from each image. The ROI was required to represent the overall color and texture features of the sample, and avoid interfering tissues such as fat and fascia<sup>[26]</sup>. ROI is extracted from the center of the sample image to both sides, and each sample extracts three different ROI images. Sample images with large deviations from other images acquired on the same day were removed. Finally, 1254 ROI images were obtained. The procedure for image processing is depicted in Figure 2.

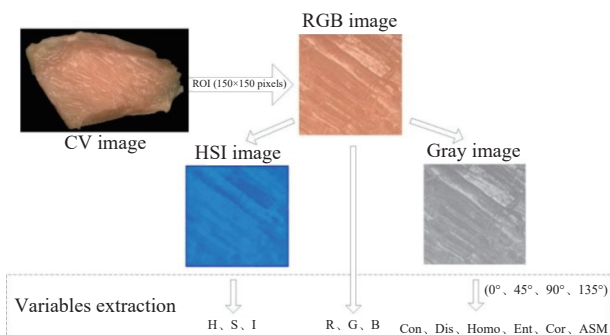


Figure 2 Extraction of image feature variables

**2.2.2 Texture feature extraction**

In the field of food inspection, image feature extraction usually starts from two aspects: color and texture. Color features are mainly used to describe changes in the external surface characteristics of food, while texture features mainly involve differences in the surface of food caused by factors such as water loss. There is an excellent theoretical basis for analyzing the freshness of chicken breast meat by using image texture features. Related studies show that meat freshness is closely related to the depth of surface

grooves, tissue changes, texture thickness, and distribution. Differences in surface texture can reflect changes in the intrinsic freshness of meat<sup>[27]</sup>. This study will extract six color features from two different color models, RGB (Red, Green, Blue) model and HSI (Hue, Saturation, Intensity) model, and calculate six main Gray Level Co-occurrence Matrix (GLCM) texture feature parameters from four directions, which are used to analyze the texture feature parameters of the chicken surface.

GLCM is a well-established statistical image analysis method that has been used in many texture-related applications<sup>[28]</sup>. The co-occurrence matrix is first calculated from the gray image, and then some eigenvalues of the matrix are obtained by calculating the co-occurrence matrix to represent some texture features of the image. GLCM can reflect comprehensive information on the image's gray direction, adjacent interval, and variation amplitude. Equation (1) is used to normalize the matrix.

$$P(i, j, d, \theta) = \frac{P(i, j)}{\sum_i \sum_j P(i, j)} \tag{1}$$

where,  $i$  and  $j$  are pixel points of matrix  $P$ ;  $d$  is distance and  $\theta$  is direction;  $P(i, j)$  is the number of symbiotic pixel points.

The grayscale size of the image determines the value of  $(i, j)$ , and  $\theta$  is the angle values for four directions, namely  $0^\circ$ ,  $45^\circ$ ,  $90^\circ$ , and  $135^\circ$ . In the GLCM, 14 possible attributes can be obtained from 4 different directions and 2 offset points. After calculating the matrix, texture features are calculated based on the co-occurrence matrix to improve image classification efficiency instead of directly applying the computed GLCM. The depth of grooves, tissue changes, texture thickness, and distribution on the surface of meat products can well reflect the freshness of the meat<sup>[29]</sup>. The following six most representative image texture features are selected in this study: contrast, dissimilarity, homogeneity, entropy, correlation, and Angular Second Moment (ASM).

1) Contrast

Contrast reflects the clarity of the image and the depth of grooves in the texture. Deeper texture grooves give greater contrast and a clearer visual effect. A larger grayscale difference gives higher values due to more pairs of pixels with large contrast. The larger the element value far away from the diagonal in the gray common generation matrix, the larger the contrast. The contrast value is calculated by Equation (2).

$$f_{con} = \sum_i \sum_j (i, j)^2 P(i, j) \tag{2}$$

2) Dissimilarity

The measurement of dissimilarity is similar to contrast, but dissimilarity is better for measuring local features. When local contrast increases, the dissimilarity also increases. The weight increases exponentially with the distance between the matrix elements and the diagonal. If the weight increases linearly, the dissimilarity is obtained. The dissimilarity value  $f_{dis}$  is calculated by Equation (3).

$$f_{dis} = \sum_i \sum_j P(i, j) * |i - j| \tag{3}$$

3) Homogeneity

Homogeneity reflects the balance moment of image texture and measures the local variation of image texture. A large homogeneity value indicates that there is little change between different areas of the image texture, and the local area is uniform. The homogeneity

value  $f_{\text{homo}}$  is calculated by Equation (4).

$$f_{\text{homo}} = \sum_i \sum_j (i, j)^2 \frac{P(i, j)}{1 + (i - j)^2} \quad (4)$$

#### 4) Entropy

Entropy reflects the degree of inhomogeneity or complexity of the texture in the image. A more orderly texture gives lower entropy. Entropy also represents the information content of the image. When all elements in the co-occurrence matrix have maximum randomness, all values in the spatial co-occurrence matrix are almost equal. The entropy value  $f_{\text{ent}}$  is calculated by Equation (5).

$$f_{\text{ent}} = \sum_i \sum_j P(i, j) \log P(i, j) \quad (5)$$

#### 5) Correlation

Correlation measures the degree of similarity between spatial GLCM elements in the direction of a row or column. Therefore, the size of the correlation value reflects the local gray-level correlation in the image. When the matrix element values are equal, the correlation value is large. On the contrary, if the matrix pixel values are very different, the correlation value is small. If there is a horizontal texture in the image, the correlation of the horizontal matrix is greater than the correlation values of the other matrix. The correlation value  $f_{\text{cor}}$  is calculated by Equation (6).

$$f_{\text{cor}} = \sum_i \sum_j \frac{(i - u_x)(i - u_y)P(i, j)}{\sigma_x \sigma_y} \quad (6)$$

#### 6) ASM

ASM is the sum of squares of the element values of the GLCM, and is also called the energy, which reflects the uniformity of image gray distribution and texture thickness. A large ASM value indicates a more uniform and regular texture pattern. The ASM value  $f_{\text{ASM}}$  is calculated by Equation (7).

$$f_{\text{ASM}} = \sum_i \sum_j P(i, j)^2 \quad (7)$$

For each image, the original is a color image with three channels, and each channel has values of 0-255.

To reduce the amount of calculation, each component is quantified to 16 grayscale levels when extracting features. Although the accuracy of the simplified image information is slightly reduced, this does not affect the extraction of texture features. Due to the irregular texture distribution of chicken breast images, four directions of  $0^\circ$ ,  $45^\circ$ ,  $90^\circ$ , and  $135^\circ$  were taken for an average calculation to minimize the influence of different directions on texture features. Finally, 24 GLCM texture feature parameters were extracted from each image to describe the texture information of the chicken breast images.

#### 2.2.3 Color feature extraction

The color of the object is often expressed in color space. RGB and HSI are considered the most representative color spaces<sup>[20]</sup>. RGB is a color space based on the display device, as shown in Figure 3. The RGB color space uses only three colors (Red, Green, Blue) to assign an intensity value in the 0 to 255 range to each pixel in the image, allowing them to be combined in different proportions to reproduce 16 777 216 ( $256 \times 256 \times 256$ ) colors on the screen.

HSI color space starts from the human visual system and describes colors with Hue, Saturation, and Intensity, as shown in Figure 3.  $I$  is the intensity axis, and the Angle range of hue ( $H$ ) is  $[0, 2\pi]$ , where the Angle of pure red is 0, the Angle of pure green is

$2\pi/3$ , and the Angle of pure blue is  $4\pi/3$ . The saturation ( $S$ ) is the distance from any point in the color space to axis  $I$ . In the field of food inspection, image feature extraction usually starts from two aspects: color and texture. Color features are mainly used to describe changes in the external surface characteristics of food, while texture features mainly involve differences in the surface of food caused by factors such as water loss<sup>[30]</sup>.

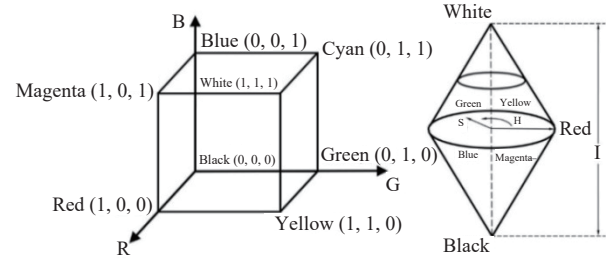


Figure 3 RGB and HSI color space

#### 2.2.4 Data dimension reduction

The 24 texture features and 6 color features of the extracted ROI image were used to describe the freshness of chicken breast samples. The mean statistical results of texture features and color features of samples, measured daily, are listed in Tables 1 and 2.

Table 1 Descriptive statistics of texture features of chicken

	meat						
Texture features	1 d	2 d	3 d	4 d	5 d	6 d	7 d
Contrast $0^\circ$	0.2418	0.2447	0.2488	0.2307	0.2400	0.2374	0.2289
Contrast $45^\circ$	0.4224	0.4599	0.4848	0.4622	0.4600	0.4683	0.4628
Contrast $90^\circ$	0.3362	0.3549	0.3650	0.3508	0.3573	0.3525	0.3571
Contrast $135^\circ$	0.4079	0.4404	0.4473	0.4294	0.4460	0.4376	0.4433
Dissimilarity $0^\circ$	0.2331	0.2264	0.2261	0.2077	0.2147	0.2123	0.2051
Dissimilarity $45^\circ$	0.3695	0.3641	0.3672	0.3419	0.3466	0.3436	0.3384
Dissimilarity $90^\circ$	0.3095	0.3035	0.3032	0.2843	0.2883	0.2840	0.2849
Dissimilarity $135^\circ$	0.3599	0.3546	0.3498	0.3270	0.3356	0.3300	0.3291
Homogeneity $0^\circ$	0.8843	0.8886	0.8890	0.8985	0.8952	0.8963	0.8998
Homogeneity $45^\circ$	0.8206	0.8275	0.8281	0.8411	0.8391	0.8406	0.8432
Homogeneity $90^\circ$	0.8479	0.8534	0.8546	0.8645	0.8628	0.8648	0.8647
Homogeneity $135^\circ$	0.8248	0.8313	0.8348	0.8467	0.8432	0.8457	0.8468
Entropy $0^\circ$	0.5487	0.5919	0.6025	0.6326	0.6222	0.6223	0.6320
Entropy $45^\circ$	0.5030	0.5530	0.5656	0.5986	0.5896	0.5901	0.5998
Entropy $90^\circ$	0.5214	0.5693	0.5814	0.6131	0.6039	0.6048	0.6125
Entropy $135^\circ$	0.5058	0.5549	0.5689	0.6016	0.5915	0.5924	0.6015
Correlation $0^\circ$	0.7909	0.8248	0.8394	0.8460	0.8520	0.8547	0.8634
Correlation $45^\circ$	0.6362	0.6745	0.6865	0.6927	0.7109	0.7146	0.7249
Correlation $90^\circ$	0.7103	0.7485	0.7626	0.7681	0.7815	0.7856	0.7885
Correlation $135^\circ$	0.6480	0.6880	0.7097	0.7175	0.7280	0.7351	0.7389
ASM $0^\circ$	0.3063	0.3579	0.3704	0.4085	0.3971	0.3985	0.4115
ASM $45^\circ$	0.2591	0.3146	0.3287	0.3682	0.3593	0.3613	0.3739
ASM $90^\circ$	0.2778	0.3325	0.3464	0.3853	0.3759	0.3782	0.3888
ASM $135^\circ$	0.2620	0.3167	0.3321	0.3718	0.3616	0.3640	0.3760

Significant multicollinearity exists among variables in high-dimensional data, which will lead to complex models, low analysis efficiency, and redundant information, and also affect the accuracy of model prediction. Principal Component Analysis (PCA) is a statistical method for linear dimensionality reduction. Through orthogonal transformation, vectors related to the components in higher dimensional space are transformed into new vectors unrelated to these components in lower dimensional space. In this way, redundant information is removed for multiple features image



fusion, and valid data is retained to achieve dimensionality reduction. PCA was conducted on the 30 indicators of texture and color in this study, and the cumulative variance contribution rate of the first four principal components reached 92.203%, which could well replace the 30 original features. Table 3 shows the contribution rates of principal component analysis using SPSS software on a total of 30 extracted image features, including color and texture parameters. PC1, PC2, PC3, and PC4 reflect 61.836%, 16.822%, 7.688%, and 5.857% of the original information, respectively. As shown in Figure 4, the principal components can better classify the three freshness levels of samples in three-dimensional space, indicating that the obtained principal components can effectively replace the 30 original features.

**Table 2 Descriptive statistics of color features of chicken meat**

Color features	1 d	2 d	3 d	4 d	5 d	6 d	7 d
<i>R</i>	120.44	126.52	123.06	120.49	115.22	115.34	117.13
<i>G</i>	81.62	89.55	89.96	90.71	87.35	88.81	88.39
<i>B</i>	58.72	59.83	58.36	57.45	56.17	55.04	55.56
<i>H</i>	8.33	10.09	11.35	12.14	12.60	13.12	12.40
<i>S</i>	16.91	20.07	21.94	23.22	22.79	24.80	23.76
<i>I</i>	62.72	68.78	68.17	67.83	67.09	66.01	66.43

**Table 3 Contribution of 30 features for multiple features image fusion**

Features	PC1	PC2	PC3	PC4
dis 45°	-0.985	-0.075	0.008	0.006
homo 45°	0.983	0.113	0.058	-0.010
homo 135°	0.979	0.090	0.068	-0.020
homo 90°	0.979	0.111	0.031	-0.014
dis 135°	-0.979	-0.054	-0.009	0.016
dis 90°	-0.978	-0.084	0.013	0.013
homo 0°	0.958	0.083	0.052	0.007
dis 0°	-0.957	-0.071	-0.028	-0.010
con 90°	-0.941	0.016	0.173	0.008
con 0°	-0.941	-0.022	0.076	-0.020
ent 90°	0.939	-0.012	0.287	0.007
ASM 90°	0.938	-0.007	0.288	-0.007
ent 0°	0.937	-0.052	0.289	0.011
ent 135°	0.936	-0.014	0.296	0.004
con 45°	-0.936	0.051	0.217	-0.007
ASM 0°	0.936	-0.045	0.290	-0.002
ASM 135°	0.935	-0.009	0.296	-0.010
ent 45°	0.935	-0.004	0.295	0.007
ASM 45°	0.933	0.001	0.294	-0.008
con 135°	-0.928	0.066	0.182	0.004
cor 45°	0.17	0.962	0.045	-0.054
cor 90°	0.050	0.952	0.109	-0.066
cor 135°	0.051	0.942	0.121	-0.064
cor 0°	-0.009	0.909	0.248	-0.037
I	0.018	0.627	0.133	0.257
H	0.069	0.337	0.889	-0.093
S	0.244	0.096	0.886	-0.131
G	0.074	0.357	0.860	0.189
B	0.012	0.138	0.197	0.926
R	-0.019	-0.159	-0.335	0.881

**2.3 Establishment of prediction model**

To predict and determine chicken freshness level, 1524 datasets were divided into training, testing, and validation sets in a ratio of

7:2:1. Six principal components obtained from principal component analysis of 30 image feature parameters were used as model inputs, and three freshness levels were used as dataset labels. The machine learning model was trained based on the set structural parameters. Additionally, prediction models were established based on the image parameters of samples, using four types of common machine learning algorithms: PSO-SVM, Random Forests (RF), Gradient Boosting Decision Tree (GBDT), and Naive Bayes Classifier (NBC).

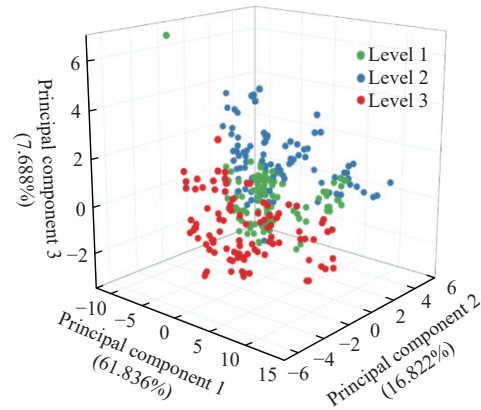


Figure 4 Visualization of principal components

1) PSO-SVM

SVM is a supervised learning model based on the principle of structural risk minimization. It constructs a hyperplane or hyperplane set in a high-dimensional or infinite-dimensional space, maps the original finite-dimensional space to a space with higher dimensions, and makes classification easier in this space.

To achieve better classification, SVM maps the input space to the high-order feature space through some linear transformation. If the low-dimensional space exists that makes the establishment of, then is called the kernel function, which is the inner product mapped to the feature space. The choice of kernel function is key to building a well-performing SVM model. There are two parts to selecting the kernel function: to select the type of kernel function, and to select the relevant parameters of the kernel function. Linear kernel function is mainly chosen in the case of linear separability, since it has a faster speed and an ideal effect on general data classification, while Radial Basis Function (RBF) is mainly chosen in the case of linear indivisibility. There are many parameters, and the classification results are highly dependent on parameters. By trialing a large number of parameters, a better effect than the linear core was generally found. A pre-classification experiment for chicken freshness was performed through the unoptimized SVM model, and the results of classifying chicken samples with different freshness levels by the SVM model with different kernel functions under the same data conditions were compared, as shown in Figure 5.

As can be seen from Figure 5, the SVM model using the RBF kernel function has a higher classification accuracy than those using the other three kernel functions. Therefore, the RBF function is adopted as the kernel function of SVM in this study. RBF kernel function has strong flexibility, and is also known as Gaussian kernel due to its similarity to the Gaussian Function, as shown in Equation (8).

$$K(x,y) = \exp\left(-\frac{\|x-y\|^2}{2\sigma^2}\right) \tag{8}$$

where a larger value results in a smoother RBF kernel function,

which changes slowly with the input. This function has poor generalization ability and is easy to overfit. A smaller value results in a more drastic change of RBF kernel function, and the model is more sensitive to noise samples.

After choosing the type of kernel function, it was also necessary to determine the penalty parameter  $C$  and the kernel function parameter  $g$ . Particle Swarm Optimization (PSO) algorithm is derived from studying the social behavior of birds or fish, and relies on the cooperation and information sharing among individuals

in the group to find the optimal solution. PSO algorithm has been widely used in function optimization because of its simple operation and fast convergence. Therefore, the PSO algorithm was adopted in this study to optimize the penalty parameter  $C$  of SVM and the kernel function parameter  $g$ . The optimization steps are shown in Figure 6. The global optimum of the final model was obtained in the 10<sup>th</sup> iteration, with the optimal penalty parameter  $C=9.95$  and the kernel function parameter  $g=0.38$ .

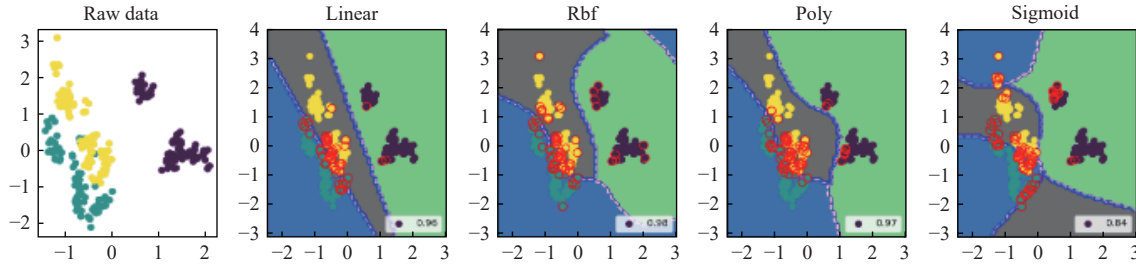


Figure 5 Classification effect of SVM model with different kernel functions

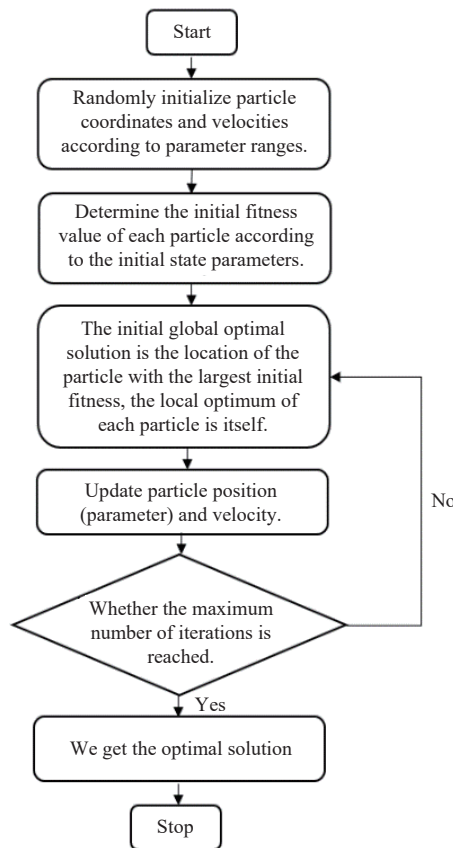


Figure 6 Flow diagram of PSO algorithm

2) Random Forest (RF)

Random Forest is an integrated algorithm specially designed for decision tree classification. It obtains a final prediction result by integrating and weighting the prediction results of multiple decision trees and is an extension of the Bagging method. RF algorithm randomly selects  $n$  attributes from all attributes each time, and then selects an optimal attribute from the  $n$  attributes as its branch attribute so that the generalization ability of the model is stronger. The selection of parameter  $n$  determines the randomness of the model. If there are a total of  $M$  sample attributes,  $n=1$  means that one attribute is selected randomly as the branching attribute, and the value of  $n$  is usually the largest integer less than  $\log_2(M+1)$ . RF

algorithm usually uses the Classification and Regression Tree algorithm (CART) as the generation and pruning algorithm of the decision tree.

The main parameters of the RF algorithm in this study were set as follows:

- (1) The maximum number of iterations for the weak learner,  $n\_estimators$ , was set to 100.
- (2) The selected feature selection criterion was “Gini”.
- (3) The minimum sample number of leaf nodes,  $min\_samples\_split$ , was set to 5.

3) Gradient Boosting Decision Tree (GBDT)

GBDT algorithm is an improvement of the gradient lifting decision tree, which uses the lifting method and combines it with multiple decision trees to make common decisions. The original Boosting algorithm attaches an equal weight value to each sample and updates the weight during the algorithm running. Using square error as GBDT algorithm error function, each regression tree learns the residuals previously accumulated by all decision trees, and establishes a new model in the gradient direction of residual reduction. It uses the loss function of the negative gradient in the value of the current model as residual ascension approximation in the tree to fit the regression decision tree. Therefore, in GBDT, the establishment of each new model reduces the residual of the previous model in the gradient direction. The GBDT algorithm model is as follows:

- (1) Initialize the decision tree, estimate a constant that minimizes the loss function, and build a tree with only the root node.
- (2) Escalating Iteration:
  - ① Calculate the negative gradient of the loss function in the current model as the estimated value of the residual.
  - ② Estimate the region of leaf nodes in the regression tree, and fit the approximate value of residual.
  - ③ Use linear search to estimate the value of leaf node region as a loss function minimization.
  - ④ Update the decision tree.
- (3) After several iterations of the lifting method, the final model is obtained as output.

In this study, the main parameters of the GBDT algorithm were set as follows:

- ① Loss function was set to “deviance”.
- ② The maximum number of iterations of the weak learner,

$n\_estimators$ , was set to 100.

③ The weight reduction coefficient learning rate of the weak learner was set to 0.1.

④ The *subsample* was set to 0.7.

⑤ The maximum depth of the weak learner, *max\_depth*, was set to 3.

#### 4) Naive Bayes Classifier (NBC)

NBC (Naive Bayes Classifier) divides the problem into eigenvariables and decision vectors. It is assumed that the eigenvariables have no correlation with each other and act independently on the decision variables. This hypothesis can make the NBC model exponentially reduce the complexity of Bayesian network construction, and well handle the noise and irrelevant attributes of the training samples.

Assuming that the eigenvariables of the problem, which are independent of each other, can be decomposed into the product of multiple vectors, as shown in Equation (9),

$$p(x|y) = \prod_{i=1}^n p(x_i|y) \quad (9)$$

then the problem can be solved by using simple NBC, as shown in Equation (10).

$$p(y|x) = \frac{p(y) \prod_{i=1}^n p(x_i|y)}{p(x)} \quad (10)$$

where,  $p(x)$  is treated as constant, and the prior probability can be estimated by the proportion of each type of sample in the training set. Given the condition, if the classification of test samples is to be estimated, the posterior probability is obtained by NBC, as shown in Equation (11).

$$p(y = Y|x) = \frac{p(y = Y) \prod_{i=1}^n p(x_i|y = Y)}{p(x)} \quad (11)$$

Finally, the largest category  $y$  is needed for  $p(y = Y) \prod_{i=1}^n p(x_i|y = Y)$  to be found.

## 3 Results and discussion

### 3.1 Experimental conditions and configuration

The software platforms used in this experiment were Pycharm2019.3, OpenCV-Python 4.5.1, torch1.7.0+cuda11.0, and torch vision 0.8.1+cuda11.0.

The hardware platform used was Dell Inspiron15-7572 (Intel Core i5 8th Gen, Computer Memory - 8 GB). Connect to the cloud host during training; the cloud host was GeForce RTX 2080 Ti with 11 GB Video Memory.

### 3.2 Detection results

#### 3.2.1 Network initialization parameters

In our experiment, four principal components obtained by PCA of 30 original feature parameters were used as model input, and three chicken freshness levels were used as labels. Following this, four machine learning models were trained according to the set structure parameters.

The division of the training set and the test set used the k-fold cross-validation, where  $K=10$  was selected in this study. The dataset was randomly divided into 10 folds, where the dataset of each fold was selected as the validation set and the rest as the training set. The division of the training set and test set was changed, the model was

trained and verified many times, and the average of  $K$  records was taken as the final result.

The statistical results of the experiment are listed in Table 4. Compared with the other three models Random Forest, GBDT, and NBC, the accuracy of the PSO-SVM model is relatively higher, reaching 0.9867. Here, SVM has the advantage of being able to solve nonlinear problems and deal with small samples. In the SVM model, the samples are expected to be linearly separable in the feature space, so the quality of the feature space is very important for the performance of the support vector machine. It is worth noting that when the form of feature mapping is unknown, the appropriate kernel function is unknown, so the selection of kernel function becomes the biggest variable of SVM. In the study, the classification effects of four different kernel functions were compared in SVM. After determining the use of RBF as the kernel function, the PSO algorithm was used to solve its key parameters, and finally obtained the SVM model suitable for this project. It should be mentioned that the accuracy of the other three models were all above 0.94. Figure 7 shows the classification and recognition results of the four models in the sample test set.

**Table 4 Prediction Results**

Model	Accuracy Rate		
	Training	10-fold CV	Detection
PSO-SVM	0.9904	0.9867	0.9889
Random Forest	0.9856	0.9733	0.9667
GBDT	0.9713	0.9433	0.9556
Naive Bayes Classifier	0.9522	0.9433	0.9556

From Figure 7, it can be seen that RF, GBDT, and NBC have low recognition accuracy for third-level freshness samples, and there is a phenomenon of missed detections. However, there is almost no missed detection phenomenon in PSO-SVM. The results prove the feasibility of using machine vision technology combined with machine learning methods to classify and predict chicken freshness, and illustrate the importance of using color features together with texture features in this process. Furthermore, the PSO-SVM performs excellently.

#### 3.2.2 Discussion

It is evident from the experimental results that visual technology has great potential for application in the non-destructive detection of meat quality. Compared with traditional manual detection methods, our method of combining visual technology and machine learning provides significantly higher accuracy and speed. Moreover, this method only needs to collect the image features of the sample without damaging the sample, which is of great significance from a sustainability perspective and advantageous for the gradual promotion of this method to the market. Of course, before our detection method can be practically applied in an industrial setting, it is necessary to optimize the performance of the classification model and enhance its robustness, such that the model can provide higher classification accuracy even under unstable lighting or other conditions in the factory, to meet the needs of modern production.

Before determining the final experimental design, the methods used by other researchers were compared and analyzed for meat quality detection. Visual technology based on visible light color images has had the longest history of application. This method has further evolved with rapid developments of industrial cameras, image processing, and pattern recognition technology. Compared with existing research, the method proposed which utilized the color

and texture information of the image has the advantages of a simple device structure, a relatively small workload of data processing, and a high accuracy of classifying chicken freshness (maximum of

0.9867). The results suggest that this method has great application value and potential in the non-destructive detection of meat quality in industrial production.

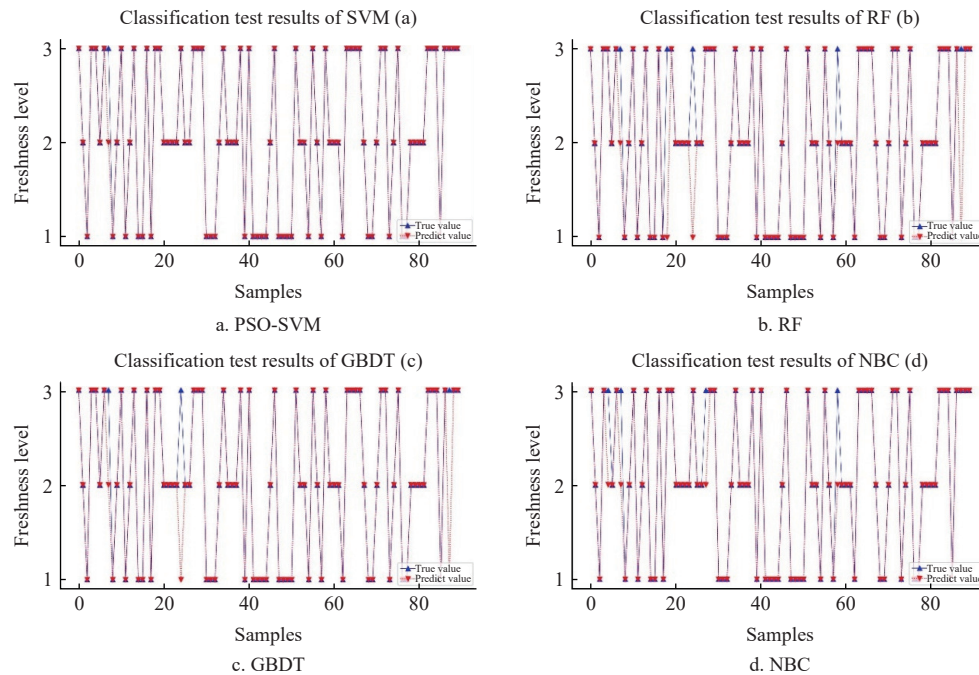


Figure 7 Classification test results

## 4 Conclusions

A self-designed machine vision system was used to collect images of chicken breasts, and six color features were extracted from two different color spaces (RGB, HSI) in the ROI of images. The Gray-Level Co-occurrence Matrix was calculated, using the six main texture features of contrast, dissimilarity, homogeneity, entropy, correlation, and ASM. PCA was used to reduce the dimensionality of 30 extracted parameters for multiple features image fusion, and four principal components were obtained. Four types of machine learning algorithms, SVM, Random Forest, GBDT, and NBC, were used to establish the chicken freshness level prediction model based on principal components. Through analysis and comparison, the prediction effect of the SVM model was found to be the best, where the prediction accuracy of the model test set reached 0.9867. This study provides a theoretical basis for more extensive research on predicting chicken freshness using visual technology and machine learning and has a practical guiding role in developing a comprehensive evaluation framework and the industrial application of non-destructive online detection.

In future research, the addition of an electronic nose device built by our laboratory will be investigated in this project. The electronic nose will allow the collection and processing of chicken odor information to obtain the maximum response value, baseline value, area integral, and other feature values of the sensor response curve. By combining odor information with image information to perform multi-source data fusion, more comprehensive and accurate characterization of chicken quality is anticipated to be achieved. This method can further address a common limitation of current research methods for analyzing meat samples based solely on image information, which has high requirements for the environment of image collection. Particularly when the image quality is low, the electronic nose sensor data can supplement the image data to ensure or enhance the accuracy of classification. The combinatorial

strategy illustrated in this study, integrating multiple sources of sample information, has great potential to be adapted and applied in the quality detection of various foods in the future, not necessarily limited to meat products. This study has great research significance for new methods to improve the assessment of food quality and safety in industrial applications.

## Acknowledgements

This research was funded by the International Science and Technology Cooperation Program of Jiangsu Province (Grant No. BZZ2023013) and the Xuzhou Key Research and Development Project (Modern Agriculture) (Grant No. KC21135).

## [References]

- [1] Govoni C, Chiarelli DD, Luciano A, Ottoboni M, Perpelek SN, Pinotti L, et al. Global assessment of natural resources for chicken production. *Advances in Water Resources*, 2021; 154: 103987.
- [2] Sujiwo J, Kim D, Jang A. Relation among quality traits of chicken breast meat during cold storage: correlations between freshness traits and torrymeter values. *Poultry Science*, 2018; 97(8): 2887–2894.
- [3] Wang H, He H J, Ma H J, Chen F S, Kang Z L, Zhu M M, et al. LW-NIR hyperspectral imaging for rapid prediction of TVC in chicken flesh. *Int J Agric & Biol Eng*, 2019; 12(3): 180–186.
- [4] Mafi G, Nair M, Hunt M, Denzer M, Suman S, Ramanathan R, et al. Recent updates in meat color research: integrating traditional and high-throughput approaches. *Meat and Muscle Biology*, 2020; 4(2): 7.
- [5] Jiang S Q, He H J, Ma H J, Chen F S, Xu B C, Liu H, et al. Quick assessment of chicken spoilage based on hyperspectral NIR spectra combined with partial least squares regression. *Int J Agric & Biol Eng*, 2021; 14(1): 243–250.
- [6] Smith M, Smith L, Hansen M. The quiet revolution in machine vision—a state-of-the-art survey paper, including historical review, perspectives, and future directions. *Computers in Industry*, 2021; 130: 103472.
- [7] Sabzi S, Javadikia H, Arribas J. A three-variety automatic and non-intrusive computer vision system for the estimation of orange fruit pH value. *Measurement*, 2019; 152: 107298.
- [8] Yang X, Liu, G, He J, Kang N, Yuan R, Fan N. Determination of sugar



- content in Lingwu jujube by NIR-hyperspectral imaging. *Journal of Food Science*, 2021; 86(4): 1201–1214.
- [9] Jin X, Li R, Tang Q, Wu J, Jiang L, Wu C. Low-damage transplanting method for leafy vegetable seedlings based on machine vision. *Biosystems Engineering*, 2022; 220: 159–171.
- [10] Palumbo M, Cefola M, Pace B, Attolico G, Colelli G. Computer vision system based on conventional imaging for non-destructively evaluating quality attributes in fresh and packaged fruit and vegetables. *Postharvest Biology and Technology*, 2023; 200: 112332.
- [11] Chen D, Wu P, Wang K, Wang S, Ji X, Shen Q, et al. Combining computer vision score and conventional meat quality traits to estimate the intramuscular fat content using machine learning in pigs. *Meat Science*, 2022; 185: 108727.
- [12] Sánchez C, Orvañanos-Guerrero M, Domínguez-Soberanes J, Alvarez-Cisneros Y. Analysis of beef quality according to color changes using computer vision and white-box machine learning techniques. *Heliyon*, 2023; 9(7): e17976.
- [13] Brand W, Wells A, Smith S, Denholm S, Wall E, Coffey M. Predicting pregnancy status from mid-infrared spectroscopy in dairy cow milk using deep learning. *Journal of Dairy Science*, 2021; 104(4): 4980–4990.
- [14] Zong W J, Xu H Y, Zhi W, Rui R Y, Rui B W. Automatic lameness detection in dairy cows based on machine vision. *Int J Agric & Biol Eng*, 2023; 16(3): 217–224.
- [15] Arsalane A, El Barbri N, Tabyaoui A, Klilou A, Rhofir K, Halimi A. An embedded system based on DSP platform and PCA-SVM algorithms for rapid beef meat freshness prediction and identification. *Computers and Electronics in Agriculture*, 2018; 152: 385–392.
- [16] Tang Y W Y, Wang X W, Xing X Y, Li Z, Zhao M C. Prediction and evaluation method of TVB-N values distribution in pork by hyperspectral imaging. *Int J Agric & Biol Eng*, 2021; 14(4): 270–276.
- [17] Luo X, Xiong L, Gao X, Hou Y, He M, Tang X. Determination of beef tenderness based on airflow pressure combined with structural light three-dimensional (3D) vision technology. *Meat Science*, 2023; 202: 109206.
- [18] He H, Wu D, Sun D. Potential of hyperspectral imaging combined with chemometric analysis for assessing and visualising tenderness distribution in raw farmed salmon fillets. *Journal of Food Engineering*, 2014; 126: 156–164.
- [19] Feng C, Makino Y, Yoshimura M, Thuyet D, García-Martín J. Hyperspectral imaging in tandem with R statistics and image processing for detection and visualization of pH in Japanese big sausages under different storage conditions. *Journal of Food Science*, 2018; 83(2): 358–366.
- [20] Sun X, Young J, Liu J, Bachmeier L, Somers R, Chen K, et al. Prediction of pork color attributes using computer vision system. *Meat Science*, 2016; 113: 62–64.
- [21] Barbin D, Mastelini S, Barbon S, Campos G, Barbon A, Shimokomaki M. Digital image analyses as an alternative tool for chicken quality assessment. *Biosystems Engineering*, 2016; 144: 85–93. doi: 10.1016/j.biosystemseng.2016.01.015.
- [22] Jo K, Lee S, Jeong S, Lee D, Jeon H, Jung S. Hyperspectral imaging-based assessment of fresh meat quality: Progress and applications. *Microchemical Journal*, 2024; 197: 109785.
- [23] Tang X, Rao L, Xie L, Yan M, Chen Z, Liu S. Quantification and visualization of meat quality traits in pork using hyperspectral imaging. *Meat Science*, 2023; 196: 109052.
- [24] Xiong Y, Li Y, Wang C, Shi H, Wang S, Yong C, et al. Non-destructive detection of chicken freshness based on electronic nose technology and transfer learning. *Agriculture*, 2023; 13(2): 496. doi: org/10.3390/agriculture13020496.
- [25] Tsafrakidou P, Sameli N, Bosnea L, Chorianopoulos N, Samelis J. Assessment of the spoilage microbiota in minced free-range chicken meat during storage at 4 C in retail modified atmosphere packages. *Food Microbiology*, 2021; 99: 103822.
- [26] Liu X, Yuan P, Li R, Zhang D, An J, Ju J, et al. Predicting breast cancer recurrence and metastasis risk by integrating color and texture features of histopathological images and machine learning technologies. *Computers in Biology and Medicine*. 2022; 146: 105569. doi: 10.1016/j.combiomed.2022.105569.
- [27] Schreuders F, Schlangen M, Kyriakopoulou K, Boom R, van der Goot AJ. Texture methods for evaluating meat and meat analogue structures: A review. *Food Control*, 2021; 127: 108103.
- [28] Jiang H, Yoon S, Zhuang H, Wang W, Li Y, Yang Y. Integration of spectral and textural features of visible and near-infrared hyperspectral imaging for differentiating between normal and white striping broiler breast meat. *Spectrochimica Acta Part A: Molecular and Biomolecular Spectroscopy*, 2019; 213: 118–126.
- [29] Zhao H T, Feng Y Z, Chen W, Jia G F. Application of invasive weed optimization and least square support vector machine for prediction of beef adulteration with spoiled beef based on visible near-infrared (Vis-NIR) hyperspectral imaging. *Meat Science*, 2019; 151: 75–81.
- [30] Liu D, Pu H B, Sun D W, Wang L, Zeng X A. Combination of spectra and texture data of hyperspectral imaging for prediction of pH in salted meat. *Food Chemistry*, 2014; 160: 330–337.